

Complete elastic solution of pressurized thick cylindrical shells made of heterogeneous functionally graded materials

Mehdi Ghannad*, Mohammad Zamani Nejad**

*Mechanical Engineering Faculty, Shahrood University of Technology, Shahrood, Iran,

E-mail: ghannad.mehdi@gmail.com

**Mechanical Engineering Department, Yasouj University, Yasouj P. O. Box: 75914-353 Iran,

E-mail: m.zamani.n@gmail.com

crossref <http://dx.doi.org/10.5755/j01.mech.18.6.3158>

1. Introduction

Recently, a new category of composite materials known as heterogeneous composite materials has attracted interest of many researchers. Heterogeneous composite materials are functionally graded materials (FGMs) with gradient compositional variation of the constituents from one surface of the material to the other which results in continuously varying material properties. These materials are advanced, heat resisting, erosion and corrosion resistant, and have high fracture toughness. The FGMs concept is applicable to many industrial fields such as aerospace, nuclear energy, chemical plant, electronics, biomaterials and so on.

For a homogeneous hollow annular disk or tube, the elastic behavior of this class of structures subjected to external pressure is well-known [1]. Fukui and Yamanaka [2] used the plane elasticity theory (PET) for the derivation of governing equation of a thick-walled FGM tube under internal pressure and solved the obtained equation numerically by means of the Runge-Kutta method. Closed-form solutions are obtained by Tutuncu and Ozturk [3] for cylindrical and spherical vessels with variable elastic properties obeying a simple power law through the wall thickness which resulted in simple Euler-Cauchy equations whose solutions were readily available. A similar work was also published by Horgan and Chan [4] where it was noted that increasing the positive exponent of the radial coordinate provided a stress shielding effect whereas decreasing it created stress amplification. Hongjun et al. [5] and Zhifei et al. [6] provided elastic analysis and exact solution for stresses in FGM hollow cylinders in the state of plane strain with isotropic multi-layers based on Lamé's solution. Given the assumption that the material is isotropic with constant Poisson's ratio and exponentially varying Young's modulus through the thickness, Tutuncu [7] obtained power series solutions for stresses and displacements in functionally-graded cylindrical vessels subjected to internal pressure alone. Using Airy stress function, Nie and Batra [8] are obtained analytical solutions for plane strain static deformations of a functionally graded (FG) hollow circular cylinder. Zamani Nejad et al. [9] developed 3-D set of field equations of FGM thick shells of revolution in curvilinear coordinate system by tensor calculus. Ghannad and Zamani Nejad [10] present the general method of derivation and the analysis of an internally pressurized thick-walled cylinder shell with clamped-clamped ends.

The main objective of this paper is to present a

complete closed-form solution for pressurized FGM thick-walled cylindrical shells. The analytical solution is obtained for all roots of Navier equation in plane strain and plane stress conditions.

2. Basic formulations of the problem

Consider a thick hollow FGM cylinder with an inner radius r_i , and an outer radius r_o , subjected to internal and external pressure P_i and P_o , respectively.

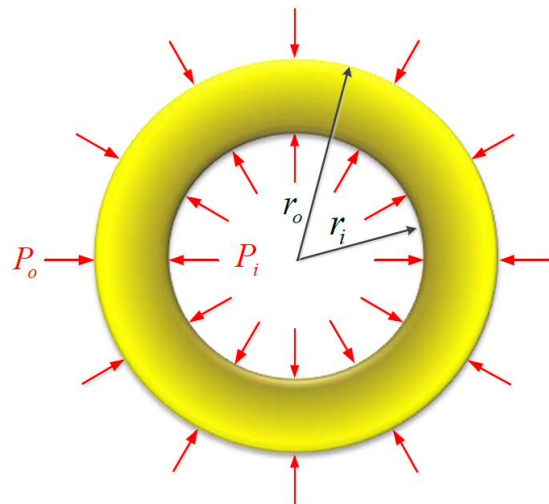


Fig. 1 Cross-section of thick cylinder

The PET is based on the assumption that the straight lines perpendicular to the central axis of the cylinder remain unchanged after loading and deformation. According to this theory, the deformations are axisymmetric and do not change along the longitudinal cylinder. In other words, the radial deformation is dependent only on radius ($u_r(r)$). In addition, normal stresses are principal stresses.

For an inhomogeneous thick hollow cylinder, the axisymmetric radial and circumferential stresses σ_r and σ_θ are dependent on r . They satisfy the following equilibrium equation in cylindrical coordinates,

$$\frac{d\sigma_r}{dr} + \frac{1}{r}(\sigma_r - \sigma_\theta) = 0 \quad (1)$$

where the body force has been neglected.

To obtain the distribution of σ_r and σ_θ , they are expressed in terms of a single radial displacement component u_r by the constitutive equations of non-homogenous

and isotropic materials

$$\begin{Bmatrix} \sigma_r \\ \sigma_\theta \end{Bmatrix} = E(r) \begin{bmatrix} A & B \\ B & A \end{bmatrix} \begin{Bmatrix} \varepsilon_r \\ \varepsilon_\theta \end{Bmatrix} \quad (2)$$

where E is Young's modulus and given the ending conditions A and B are related to Poisson's ratio, ν , and

$$\begin{Bmatrix} \varepsilon_r = \frac{du_r}{dr} \\ \varepsilon_\theta = \frac{u_r}{r} \end{Bmatrix} \quad (3)$$

where ε_r and ε_θ are radial strain and circumferential strain, respectively. Axial stress in the thick cylindrical shells is defined as follows

$$\sigma_x = \alpha(\sigma_r + \sigma_\theta) \quad (4)$$

here α is dependent on end conditions.

A case is considered in which the Young's modulus E has a power-law dependence on the radial coordinate, while the Poisson's ratio ν is a constant value.

The radial coordinate r is normalized as $\bar{r} = r/r_i$. The Young's modulus through the wall thickness is assumed to vary as follows

$$E(r) = E_i(\bar{r})^n \quad (5)$$

here E_i is the Young's modulus at the inner surface $r = r_i$, and n is the inhomogeneity constant determined empirically.

Substitution of Eqs. (3) and (5) into Eq. (2), and the use of Eq. (1) lead to the Navier equation

$$r^2 \frac{d^2 u_r}{dr^2} + (n+1)r \frac{du_r}{dr} + (n\nu^* - 1)u_r = 0 \quad (6)$$

where $\nu^* = B/A$ and given the ending conditions of the cylinder, it is determined. Substituting $u_r(r) = r^m$ in Eq. (6), the characteristic equation is obtained as follows,

$$m^2 + (n+1)m + (n\nu^* - 1) = 0 \quad (7)$$

The roots of characteristic equation are

$$\begin{Bmatrix} m_{1,2} = \frac{1}{2}(-n \pm \sqrt{\Delta}) \\ \Delta = n^2 - 4(n\nu^* - 1) \end{Bmatrix} \quad (8)$$

These roots may be (a) real, (b) double, (c) complex conjugate.

3. Ending conditions of the cylinder

The distribution of stresses and displacement in a thick-walled cylinder in the conditions of plane stress, plane strain and a cylinder with closed ends will be calculated. In each of the above-mentioned conditions, the coef-

ficients of A and B are expressed as follows:

1) plane stress (cylinder with open ends),
 $\sigma_x = 0, \varepsilon_x \neq 0$

$$\begin{Bmatrix} A = \frac{1}{1-\nu^2} \\ B = \frac{\nu}{1-\nu^2} \end{Bmatrix} \quad (9)$$

2) plane strain (Cylinder with closed ends and constrained), $\sigma_x \neq 0, \varepsilon_x = 0$

$$\begin{Bmatrix} A = \frac{1-\nu}{(1+\nu)(1-2\nu)} \\ B = \frac{\nu}{(1+\nu)(1-2\nu)} \end{Bmatrix} \quad (10)$$

3) cylinder with closed ends and non-constrained,
 $\sigma_x \neq 0, \varepsilon_x \neq 0$:

$$\begin{Bmatrix} A = \frac{2-\nu}{2(1+\nu)(1-2\nu)} \\ B = \frac{3\nu}{2(1+\nu)(1-2\nu)} \end{Bmatrix} \quad (11)$$

For homogeneous and nonhomogeneous thick cylindrical shells, the (1) and (2) conditions are used. The condition (3) is used only for homogeneous thick cylindrical shells. α in terms of different end conditions is as follows

$$\alpha = \begin{Bmatrix} 0 & \text{Plane stress} \\ \nu & \text{Plane strain} \\ 0.5 & \text{Closed cylinder} \end{Bmatrix}. \quad (12)$$

4. Solution for heterogeneous thick cylinder

Now, Eq. (6) for real, double and complex roots will be solved given the cylinder ending conditions. Following that, in each of the conditions, parametric equations of radial stress, circumferential stress and radial displacement will be derived.

4.1. Real roots

In this case, $\Delta > 0$ and we have,

$$\begin{Bmatrix} m_1 = -\frac{n}{2} + \frac{\sqrt{\Delta}}{2} \\ m_2 = -\frac{n}{2} - \frac{\sqrt{\Delta}}{2} \end{Bmatrix} \quad (13)$$

and

$$\Delta = n^2 - 4(n\nu^* - 1) \quad (14)$$

The solution of Eq. (6) is as follows

$$u_r(r) = C_1 r^{m_1} + C_2 r^{m_2} \quad (15)$$

Substituting Eq. (15) into Eq. (3) and the use of Eq. (2), the radial stress is obtained as

$$\sigma_r = E_i(\bar{r})^n \left[C_1 (Am_1 + B) r^{m_1-1} + C_2 (Am_2 + B) r^{m_2-1} \right] \quad (16)$$

For a cylinder subjected to internal and external pressure, constants C_1 and C_2 are determined using boundary conditions as

$$\left. \begin{aligned} \sigma_r|_{\bar{r}=1} &= -P_i \\ \sigma_r|_{\bar{r}=k} &= -P_o \end{aligned} \right\} \quad (17)$$

Thus

$$\sigma_r = \frac{(\bar{r})^{n-1}}{k^{m_1} - k^{m_2}} \left[(k^{m_2} P_i - k^{1-n} P_o)(\bar{r})^{m_1} - (k^{m_1} P_i - k^{1-n} P_o)(\bar{r})^{m_2} \right] \quad (20)$$

$$\sigma_\theta = \frac{(\bar{r})^{n-1}}{k^{m_1} - k^{m_2}} \left[\frac{A + Bm_1}{Am_1 + B} (k^{m_2} P_i - k^{1-n} P_o)(\bar{r})^{m_1} - \frac{A + Bm_2}{Am_2 + B} (k^{m_1} P_i - k^{1-n} P_o)(\bar{r})^{m_2} \right] \quad (21)$$

$$u_r = \frac{r_i}{E_i(k^{m_1} - k^{m_2})} \left[\frac{1}{Am_1 + B} (k^{m_2} P_i - k^{1-n} P_o)(\bar{r})^{m_1} - \frac{1}{Am_2 + B} (k^{m_1} P_i - k^{1-n} P_o)(\bar{r})^{m_2} \right] \quad (22)$$

It could be seen that radial stress does not depend on A and B . Rather, it depends on v^* and n . Circumferential stress and radial displacement are dependent on A and B .

The value of effective stress based on von Mises failure theory is as follows

$$\sigma_{eff} = \frac{1}{\sqrt{2}} \left[(\sigma_r - \sigma_\theta)^2 + (\sigma_\theta - \sigma_x)^2 + (\sigma_x - \sigma_r)^2 \right]^{0.5} \quad (23)$$

With Substituting Eq. (4) into Eq. (23), the

a) plane stress

$$\sigma_\theta = \frac{(\bar{r})^{n-1}}{k^{m_1} - k^{m_2}} \left[\frac{1 + \nu m_1}{m_1 + \nu} (k^{m_2} P_i - k^{1-n} P_o)(\bar{r})^{m_1} - \frac{1 + \nu m_2}{m_2 + \nu} (k^{m_1} P_i - k^{1-n} P_o)(\bar{r})^{m_2} \right] \quad (25)$$

$$u_r = \frac{(1 - \nu^2) r_i}{E_i(k^{m_1} - k^{m_2})} \left[\frac{1}{m_1 + \nu} (k^{m_2} P_i - k^{1-n} P_o)(\bar{r})^{m_1} - \frac{1}{m_2 + \nu} (k^{m_1} P_i - k^{1-n} P_o)(\bar{r})^{m_2} \right] \quad (26)$$

$$\sigma_{eff} = (\sigma_r^2 + \sigma_\theta^2 - \sigma_r \sigma_\theta)^{0.5} \quad (27)$$

b) plane strain

$$\sigma_\theta = \frac{(\bar{r})^{(n-1)}}{k^{m_1} - k^{m_2}} \left[\frac{(1 - \nu) + \nu m_1}{(1 - \nu) m_1 + \nu} (k^{m_2} P_i - k^{1-n} P_o)(\bar{r})^{m_1} - \frac{(1 - \nu) + \nu m_2}{(1 - \nu) m_2 + \nu} (k^{m_1} P_i - k^{1-n} P_o)(\bar{r})^{m_2} \right] \quad (28)$$

$$u_r = \frac{(1 + \nu)(1 - 2\nu) r_i}{E_i(k^{m_1} - k^{m_2})} \left[\frac{1}{(1 - \nu) m_1 + \nu} (k^{m_2} P_i - k^{1-n} P_o)(\bar{r})^{m_1} - \frac{1}{(1 - \nu) m_2 + \nu} (k^{m_1} P_i - k^{1-n} P_o)(\bar{r})^{m_2} \right] \quad (29)$$

$$\sigma_{eff} = \left[(1 - \nu + \nu^2)(\sigma_r^2 + \sigma_\theta^2) - (1 + 2\nu - 2\nu^2)\sigma_r \sigma_\theta \right]^{0.5} \quad (30)$$

$$\left. \begin{aligned} C_1 &= - \frac{(k^{m_2} P_i - k^{(1-n)} P_o) r_i^{1-m_1}}{E_i (Am_1 + B) (k^{m_2} - k^{m_1})} \\ C_2 &= \frac{(k^{m_1} P_i - k^{(1-n)} P_o) r_i^{1-m_2}}{E_i (Am_2 + B) (k^{m_2} - k^{m_1})} \end{aligned} \right\} \quad (18)$$

where

$$k = \frac{r_o}{r_i} \quad (19)$$

Using Eqs. (18), (2) and (15), the radial stress, circumferential stress and radial displacement are obtained that follows

Eq. (23) could be rewritten in terms of α as follows

$$\sigma_{eff} = \left[(1 - \alpha + \alpha^2)(\sigma_r^2 + \sigma_\theta^2) - (1 + 2\alpha - 2\alpha^2)\sigma_r \sigma_\theta \right]^{0.5} \quad (24)$$

Now, given the ending conditions of the cylinder, Eqs. (21) and (22) are written as follows:

In reference [3], radial and circumferential stresses are obtained in plane strain and $\Delta > 0$ conditions. The equation of radial stress has been obtained correctly while the equation of circumferential stress has been derived incorrectly. To correct Eq. (10), $(a/R)^{1-\beta}$ must be substituted by $(rR/a)^{\beta-1}$, based on the notations given in the above-mentioned paper. The corrected equation appears at the present paper.

4.2. Double roots

In Eq. (8), if $\Delta = 0$, then the equation will have double roots.

$$m_1 = m_2 = m = -\frac{n}{2} \quad (31)$$

In this case, the solution of Eq. (6) is as follows

$$u_r(r) = (C_1 + C_2 \ln r) r^m \quad (32)$$

Substituting Eq. (32) into Eq. (3) and the use of Eq. (2), the radial stress is obtained as

$$\sigma_r = E_i(\bar{r})^n \left\{ C_1 (Am + B) + C_2 [A + (Am + B) \ln r] \right\} r^{m-1} \quad (33)$$

Applying the loading conditions (Eq. (17)), the constants C_1 and C_2 are obtained

$$\left. \begin{aligned} C_1 &= -\frac{r_i^{1-m}}{E_i (Am + B)^2 \ln k} \left\{ A [P_i - k^{1-m-n} P_o] + \right. \\ &\quad \left. + (Am + B) [P_i \ln r_o - k^{1-m-n} P_o \ln r_i] \right\} \\ C_2 &= \frac{r_i^{1-m}}{E_i (Am + B) \ln k} [P_i - k^{1-m-n} P_o] \end{aligned} \right\} \quad (34)$$

C_1 and C_2 are substituted in Eq. (32) and using Eqs. (3) and (2). Thus,

$$\sigma_r = -\frac{(\bar{r})^{m+n-1}}{\ln k} \left[P_i \ln \frac{k}{\bar{r}} + k^{1-m-n} P_o \ln \bar{r} \right] \quad (35)$$

$$\sigma_\theta = \frac{(\bar{r})^{m+n-1}}{\ln k} \left\{ \frac{B^2 - A^2}{(Am + B)^2} [P_i - k^{1-m-n} P_o] - \frac{A + Bm}{Am + B} \left[P_i \ln \frac{k}{\bar{r}} + k^{1-m-n} P_o \ln \bar{r} \right] \right\} \quad (36)$$

$$u_r = -\frac{r_i (\bar{r})^m}{E_i (Am + B) \ln k} \left\{ \frac{A}{Am + B} [P_i - k^{1-m-n} P_o] + \left[P_i \ln \frac{k}{\bar{r}} + k^{1-m-n} P_o \ln \bar{r} \right] \right\} \quad (37)$$

Just as the procedure above, it could be seen that radial stress does not depend on A and B . Rather, it depends on v^* and n . Circumferential stress and radial displacement are dependent on A and B . Now, given the ending conditions of the cylinder, Eqs. (36) and (37) are written as follows:

a) plane stress

$$\sigma_\theta = -\frac{(\bar{r})^{m+n-1}}{\ln k} \left\{ \frac{1-v^2}{(m+v)^2} [P_i - k^{1-m-n} P_o] + \frac{1+v}{m+v} \left[P_i \ln \frac{k}{\bar{r}} + k^{1-m-n} P_o \ln \bar{r} \right] \right\} \quad (38)$$

$$u_r = -\frac{(1-v^2) r_i (\bar{r})^m}{E_i (m+v) \ln k} \left\{ \frac{1}{m+v} [P_i - k^{1-m-n} P_o] + \left[P_i \ln \frac{k}{\bar{r}} + k^{1-m-n} P_o \ln \bar{r} \right] \right\} \quad (39)$$

b) plane strain

$$\sigma_\theta = -\frac{(\bar{r})^{m+n-1}}{\ln k} \left\{ \frac{1-2\nu}{[(1-\nu)m+\nu]^2} [P_i - k^{1-m-n} P_o] + \frac{(1-\nu)+\nu m}{(1-\nu)m+\nu} \left[P_i \ln \frac{k}{\bar{r}} + k^{1-m-n} P_o \ln \bar{r} \right] \right\} \quad (40)$$

$$u_r = -\frac{(1+\nu)(1-2\nu) r_i (\bar{r})^m}{E_i [(1-\nu)m+\nu] \ln k} \left\{ \frac{1-\nu}{(1-\nu)m+\nu} [P_i - k^{1-m-n} P_o] + \left[P_i \ln \frac{k}{\bar{r}} + k^{1-m-n} P_o \ln \bar{r} \right] \right\} \quad (41)$$

4.3. Complex roots

In Eq. (8), if $\Delta < 0$, then the equation will have complex roots.

$$\left. \begin{aligned} m_1 &= z + iy \quad , \quad m_2 = z - iy \\ z &= -\frac{n}{2} \quad , \quad y = \frac{\sqrt{-\Delta}}{2} \quad , \quad \Delta = n^2 - 4(n\nu^* - 1) \end{aligned} \right\} \quad (42)$$

In this case, the solution of Eq. (6) is as follows

$$u_r(r) = [C_1 \cos(y \ln r) + C_2 \sin(y \ln r)] r^z \quad (43)$$

Substituting Eq. (43) into Eq. (3) and the use of Eq. (2), the radial stress is obtained as

$$\sigma_r = E_i (\bar{r})^n \left\{ C_1 [(Az + B) \cos(y \ln r) - Ay \sin(y \ln r)] + C_2 [(Az + B) \sin(y \ln r) + Ay \cos(y \ln r)] \right\} r^{z-1} \quad (44)$$

Applying the loading conditions (Eq. (17)), the constants C_1 and C_2 are obtained.

$$C_1 = -\frac{r_i^{1-z}}{E_i D \sin(y \ln k)} \left\{ (Az + B) [P_i \sin(y \ln r_o) - k^{1-z-n} P_o \sin(y \ln r_i)] + Ay [P_i \cos(y \ln r_o) - k^{1-z-n} P_o \cos(y \ln r_i)] \right\} \quad (45)$$

$$C_2 = \frac{r_i^{1-z}}{E_i D \sin(y \ln k)} \left\{ (Az + B) [P_i \cos(y \ln r_o) - k^{1-z-n} P_o \cos(y \ln r_i)] - Ay [P_i \sin(y \ln r_o) - k^{1-z-n} P_o \sin(y \ln r_i)] \right\} \quad (46)$$

where

$$D = [(Az + B)^2 + A^2 y^2] \quad (47)$$

C_1 and C_2 are substituted in Eq. (43) and using Eqs. (3) and (2). Thus,

$$\sigma_r = -\frac{(\bar{r})^{z+n-1}}{\sin(y \ln k)} \left[P_i \sin\left(y \ln \left(\frac{k}{\bar{r}}\right)\right) + k^{1-z-n} P_o \sin(y \ln \bar{r}) \right] \quad (48)$$

$$\sigma_\theta = -\frac{(\bar{r})^{z+n-1}}{D \sin(y \ln k)} \left\{ \left[(A^2 + B^2)z + AB(z^2 + y^2 + 1) \right] \left[P_i \sin\left(y \ln \frac{k}{\bar{r}}\right) + k^{1-z-n} P_o \sin(y \ln \bar{r}) \right] + \right. \\ \left. + (A^2 - B^2)y \left[P_i \cos\left(y \ln \frac{k}{\bar{r}}\right) - k^{1-z-n} P_o \cos(y \ln \bar{r}) \right] \right\} \quad (49)$$

$$u_r = -\frac{r_i (\bar{r})^z}{E_i D \sin(y \ln k)} \left\{ (Az + B) \left[P_i \sin\left(y \ln \frac{k}{\bar{r}}\right) + k^{1-z-n} P_o \sin(y \ln \bar{r}) \right] + Ay \left[P_i \cos\left(y \ln \frac{k}{\bar{r}}\right) - k^{1-z-n} P_o \cos(y \ln \bar{r}) \right] \right\} \quad (50)$$

And also as before, it could be seen that radial stress does not depend on A and B . Rather, it depends on ν^* and n . Circumferential stress and radial displacement are dependent on A and B . Now, given the ending conditions of the cylinder, Eqs. (49) and (50) are written as follows:

a) plane stress

$$\sigma_\theta = -\frac{(\bar{r})^{z+n-1}}{D \sin(y \ln k)} \left\{ \left[(1 + \nu^2)z + \nu(z^2 + y^2 + 1) \right] \left[P_i \sin\left(y \ln \frac{k}{\bar{r}}\right) + k^{1-z-n} P_o \sin(y \ln \bar{r}) \right] + \right. \\ \left. + (1 - \nu^2)y \left[P_i \cos\left(y \ln \frac{k}{\bar{r}}\right) - k^{1-z-n} P_o \cos(y \ln \bar{r}) \right] \right\} \quad (51)$$

$$u_r = -\frac{(1 - \nu^2) r_i (\bar{r})^z}{E_i D \sin(y \ln k)} \left\{ (z + \nu) \left[P_i \sin\left(y \ln \frac{k}{\bar{r}}\right) + k^{1-z-n} P_o \sin(y \ln \bar{r}) \right] + y \left[P_i \cos\left(y \ln \frac{k}{\bar{r}}\right) - k^{1-z-n} P_o \cos(y \ln \bar{r}) \right] \right\} \quad (52)$$

where

$$D = [(z + \nu)^2 + y^2] \quad (53)$$

b) plane strain

$$\sigma_\theta = -\frac{(\bar{r})^{z+n-1}}{D \sin(y \ln k)} \left\{ \left[(1 - 2\nu + 2\nu^2)z + \nu(1 - \nu)(z^2 + y^2 + 1) \right] \left[P_i \sin\left(y \ln \frac{k}{\bar{r}}\right) + k^{1-z-n} P_o \sin(y \ln \bar{r}) \right] + \right. \\ \left. + (1 - 2\nu)y \left[P_i \cos\left(y \ln \frac{k}{\bar{r}}\right) - k^{1-z-n} P_o \cos(y \ln \bar{r}) \right] \right\} \quad (54)$$

$$u_r = -\frac{(1 + \nu)(1 - 2\nu) r_i (\bar{r})^z}{E_i D \sin(y \ln k)} \left\{ [(1 - \nu)z + \nu] \left[P_i \sin\left(y \ln \frac{k}{\bar{r}}\right) + k^{1-z-n} P_o \sin(y \ln \bar{r}) \right] + \right. \\ \left. + (1 - \nu)y \left[P_i \cos\left(y \ln \frac{k}{\bar{r}}\right) - k^{1-z-n} P_o \cos(y \ln \bar{r}) \right] \right\} \quad (55)$$

where

$$D = [(1-\nu)z + \nu]^2 + [(1-\nu)y]^2. \quad (56)$$

5. Solution for thick homogenous and isotropic cylinders

In thick homogenous and isotropic cylinders, Young's modulus and Poisson's ratio are both constant. By substituting $n = 0$ into Eq. (5), homogenous materials are obtained.

$$E = \text{const.} \quad (57)$$

Using Eqs. (1) to (3) and (57), the Navier equation in terms of the displacement is

$$r^2 u_r'' + r u_r' - u_r = 0 \quad (58)$$

The solution of Eq. (58) is as follows

$$u_r(r) = C_1 r^{m_1} + C_2 r^{m_2} \quad (59)$$

The characteristic equation is obtained as follows

$$m^2 - 1 = 0 \quad (60)$$

It could be observed that the roots of characteristic equation are real (roots are in set of $\Delta > 0$).

$$\left. \begin{array}{l} m_1 = +1 \\ m_2 = -1 \end{array} \right\} \quad (61)$$

Substituting $m_1 = +1$ and $m_2 = -1$ in Eq. (59)

$$u_r(r) = C_1 r + \frac{C_2}{r} \quad (62)$$

Boundary conditions for stresses given by

$$\left. \begin{array}{l} \sigma_r|_{\bar{r}=1} = -P_i \\ \sigma_r|_{\bar{r}=k} = -P_o \end{array} \right\} \quad (63)$$

With substituting the boundary conditions, the constants of C_1 and C_2 become

$$C_1 = \frac{P_i - k^2 P_o}{E(A+B)(k^2 - 1)}, \quad C_2 = \frac{(P_i - P_o)r_o^2}{E(A-B)(k^2 - 1)} \quad (64)$$

C_1 and C_2 are substituted in Eq. (62) and using Eqs. (3) and (2). Thus,

$$\sigma_r^H = \frac{1}{k^2 - 1} \left[(P_i - k^2 P_o) - (P_i - P_o) \left(\frac{k}{\bar{r}} \right)^2 \right] \quad (65)$$

$$\sigma_\theta^H = \frac{1}{k^2 - 1} \left[(P_i - k^2 P_o) + (P_i - P_o) \left(\frac{k}{\bar{r}} \right)^2 \right] \quad (66)$$

$$u_r^H = \frac{r_i \bar{r}}{E(k^2 - 1)} \left[\left(\frac{P_i - k^2 P_o}{A+B} \right) + \left(\frac{P_i - P_o}{A-B} \right) \left(\frac{k}{\bar{r}} \right)^2 \right] \quad (67)$$

It could be seen that σ_r and σ_θ are independent of A , B and E .

That is radial and circumferential stresses in homogeneous and isotropic thick-walled cylinders subjected to constant pressure and same dimensions with different values of Young's modulus are independent of the ending conditions of the cylinder.

Radial displacement depends on A , B and E . Axial stress and radial displacement (Eq. (67)) depend on ending condition as follows:

a) plane stress

$$\sigma_x^H = 0 \quad (68)$$

$$u_r^H = \frac{r_i \bar{r}}{E(k^2 - 1)} \left[\frac{(1-\nu)(P_i - k^2 P_o) + (1+\nu)(P_i - P_o) \left(\frac{k}{\bar{r}} \right)^2}{E(k^2 - 1)} \right] \quad (69)$$

$$\sigma_{eff}^H = \left[(\sigma_r^H)^2 + (\sigma_\theta^H)^2 - \sigma_r^H \sigma_\theta^H \right]^{0.5} \quad (70)$$

b) plane strain

$$\sigma_x^H = \nu(\sigma_r + \sigma_\theta) = \frac{2\nu(P_i - k^2 P_o)}{k^2 - 1} \quad (71)$$

$$u_r^H = \frac{(1+\nu)r_i \bar{r}}{E(k^2 - 1)} \left[(1-2\nu)(P_i - k^2 P_o) + (P_i - P_o) \left(\frac{k}{\bar{r}} \right)^2 \right] \quad (72)$$

$$\sigma_{eff}^H = \left[(1-\nu+\nu^2) \left[(\sigma_r^H)^2 + (\sigma_\theta^H)^2 \right] - (1+2\nu-2\nu^2) \sigma_r^H \sigma_\theta^H \right]^{0.5} \quad (73)$$

c) cylinder with closed ends

$$\sigma_x^H = \frac{\sigma_r + \sigma_\theta}{2} = \frac{P_i - k^2 P_o}{k^2 - 1} \quad (74)$$

$$u_r^H = \frac{r_i \bar{r}}{E(k^2 - 1)} \left[\frac{(1-2\nu)(P_i - k^2 P_o) + (1+\nu)(P_i - P_o) \left(\frac{k}{\bar{r}} \right)^2}{E(k^2 - 1)} \right] \quad (75)$$

$$\sigma_{eff}^H = \frac{\sqrt{3}}{2} |\sigma_r^H - \sigma_\theta^H|. \quad (76)$$

6. Results and discussion

For a case study and investigation of the graphs obtained from the numerical results, consider a thick-walled cylinder with the internal radius of $r_i = 40$ mm, the outer radius of $r_o = 60$ mm and length of $L = 800$ mm. The Young's modulus, E_i at internal radius has the value of 200 GPa. It is also assumed that the Poisson's ratio, ν , has a constant value of 0.3. The applied internal pressure and/or external pressure are 80 MPa.

6.1. Homogeneous cylinder

Radial and circumferential stresses in homogene-

ous and isotropic cylinders are independent on the mechanical properties and ending conditions of cylinders. Axial stress is independent on mechanical property while it is dependent on ending conditions of the cylinder. Radial displacement is dependent on both of them (mechanical properties and ending conditions).

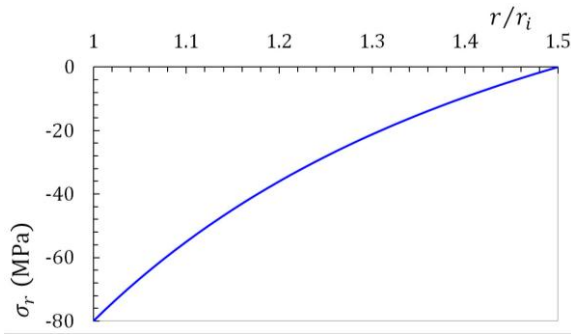


Fig. 2 Distribution of radial stress, $P_i = 80$ MPa (homogeneous cylinder)

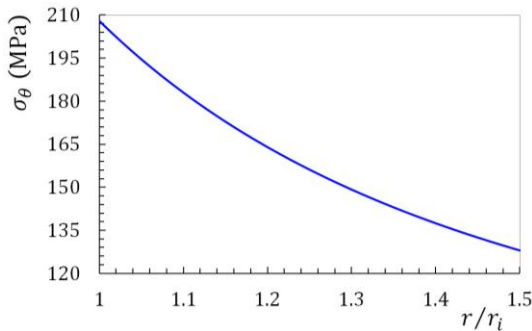


Fig. 3 Distribution of circumferential stress, $P_i = 80$ MPa (homogeneous cylinder)

Figs. 2 to 6 are plotted according to the internal pressure $P_i = 80$ MPa. Distribution of compressive radial stress based on Eq. (65), distribution of tensile circumferential stress based on Eq. (66), distribution of uniform axial stress based on Eqs. (68), (71) and (74), distribution of effective stress based on Eqs. (70), (73) and (76) are shown in Figs. 2 to 6, respectively.

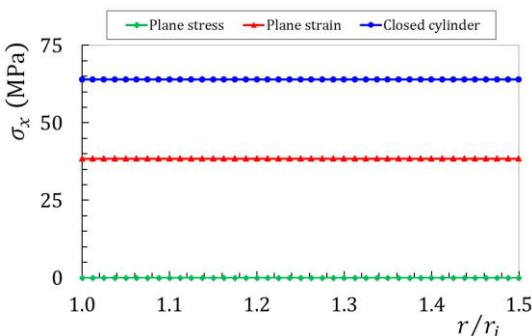


Fig. 4 Distribution of axial stress, $P_i = 80$ MPa (homogeneous cylinder)

Distribution of radial displacement based on Eqs. (69), (72) and (75) for the homogeneous cylinder is shown in Fig. 5. Figures show that the value of radial displacement is the highest for the plane stress condition and the cylinder with closed ends it is the lowest. For axial stress, the value of radial displacement is the lowest for the

plane stress condition and for the cylinder with closed ends it is the highest.

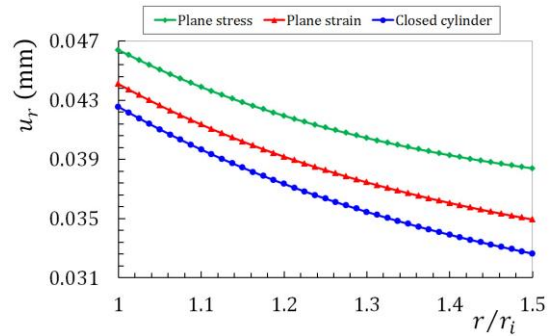


Fig. 5 Distribution of radial displacement, $P_i = 80$ MPa (homogeneous cylinder)

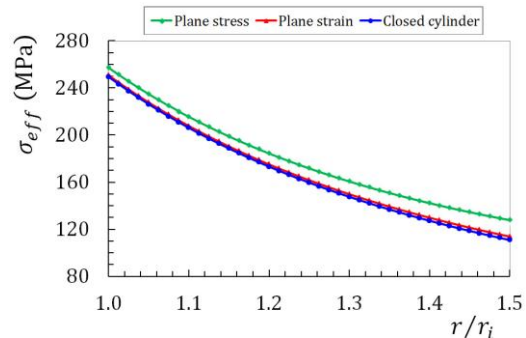


Fig. 6 Distribution of radial displacement, $P_i = 80$ MPa (homogeneous cylinder)

Distribution of von Mises effective stress, for plane strain, plane stress conditions and for the cylinder with closed ends is shown in Fig. 6. It is observed that the values of von Mises effective stress for cylinder with closed ends and for plane strain condition are close together. In addition, the value of von Mises effective stress, is the lowest for cylinder with closed ends and for plane stress condition it is the highest.

6.2. Heterogeneous cylinder

In nonhomogeneous and isotropic cylinders, radial and circumferential stresses are not independent on mechanical properties and ending conditions, rather, due to n they are dependent on mechanical properties and due to $\nu^* = B/A$ are dependent on ending conditions. Module of elasticity through the wall thickness is assumed to vary as $E(r) = E_i(\bar{r})^n$ in which the range $-2 \leq n \leq 2$ is used in the present study. In Fig. 7, for different values of n module of elasticity along the radial direction is plotted.

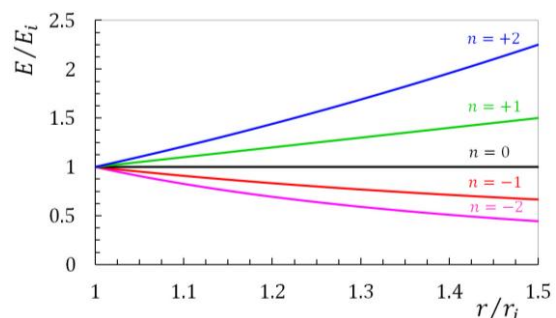


Fig. 7 Distribution of Young's modulus

The value of ν^* based on ending conditions of the cylinder is as follows:

$$\nu^* = \begin{cases} 0.3 & \text{Plane stress} \\ 0.4286 & \text{Plane strain} \end{cases} \quad (77)$$

Distribution of stresses and displacement in different ending conditions do not have significant differences, therefore, the figures are plotted for plane strain condition.

6.2.1. Internal pressure

In this section, the nonhomogeneous cylinder is only under internal pressure, $P_i = 80$ MPa.

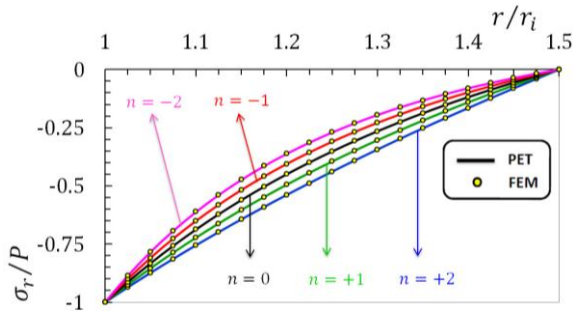


Fig. 8 Distribution of radial stress, $P_i = 80$ MPa (heterogeneous cylinder)

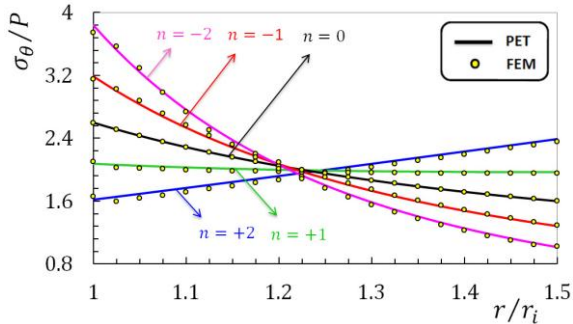


Fig. 9 Distribution of circumferential stress, $P_i = 80$ MPa (heterogeneous cylinder)

Fig. 8 shows the distribution of the compressive radial stress along the radius. The value of stress in inner and outer layers is the same, and for both layers σ_r / σ_r^H is 1. Along the radius, for $n < 0$, the radial stress decreases whereas for $n > 0$ the radial stress increases. The decrease and increase of the stress depend on $|n|$. Fig. 9 shows the distribution of the circumferential stress along the radius. The value of stress in inner and outer layers is not the same, and for both layers $\sigma_r / \sigma_\theta^H$ is not 1. The value of the circumferential stress is more than the homogeneous material for $n < 0$ in the inner half of the wall thickness while it is less than that in the outer half. This will be reverse, where $n > 0$. For $n < 0$, the circumferential stress decreases as the radius increases whereas for $n > 0$ the circumferential stress along the radius increases. The curve associated with $n = 1$ shows that the variation of circumferential stress along the radial direction is minor and is almost constant across the radius which can be an advantage in terms of stress control. It is observed that in the

range of the inner layer of the cylinder, the graphs converge and behave similarly. Fig. 10 shows the distribution of the radial displacement of the cylinder along the radius. u_r / u_r^H is not 1 at any point. For $n < 0$ the radial displacement of the cylinder is more than where the material is homogeneous and it is the reverse for $n > 0$. Yet this ratio remains almost constant along the wall thickness.

Distribution of effective stress based on Eq. (30) is shown in Fig. 11. It could be noted from this figure that at the same position, almost for $(r/r_i) < 1.2$, there is a decrease in the value of the effective stress as n increases, whereas for $(r/r_i) > 1.2$ this situation is reversed.

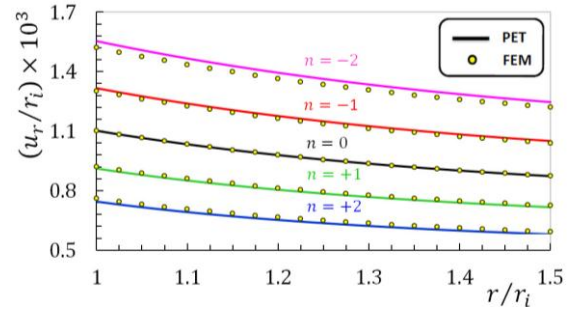


Fig. 10 Distribution of radial displacement, $P_i = 80$ MPa (heterogeneous cylinder)

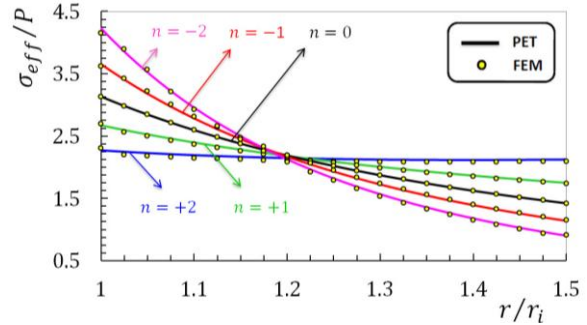


Fig. 11 Distribution of effective stress, $P_i = 80$ MPa (heterogeneous cylinder)

6.2.2. External pressure

In this section, the nonhomogeneous cylinder is only under external pressure, $P_o = 80$ MPa. The distribution of the compressive radial stress of the cylinder along the radius is shown in Fig. 12. The value of the stress in the inner and outer layers of the cylinder is the same and $\sigma_r / \sigma_r^H = 1$. In the cylinder wall the radial stress increases for $n < 0$ and decreases for $n > 0$. The magnitude of decrease or increase of the stress depends on $|n|$.

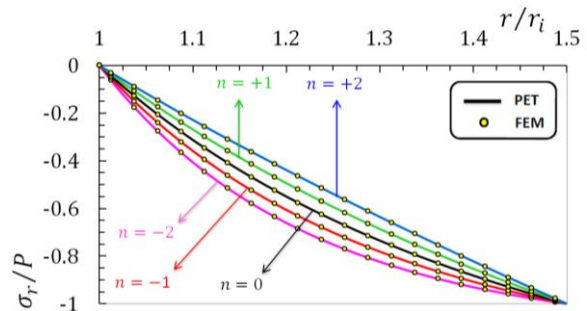


Fig. 12 Distribution of radial stress, $P_o = 80$ MPa (heterogeneous cylinder)

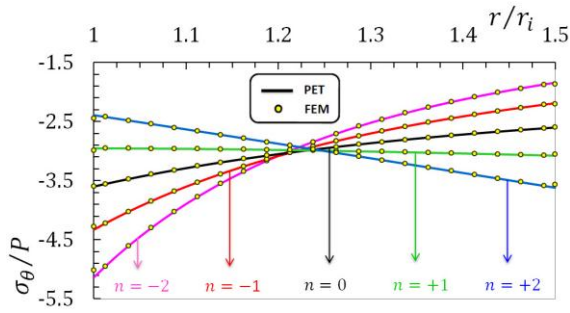


Fig. 13 Distribution of circumferential stress, $P_o = 80$ MPa (heterogeneous cylinder)

The distribution of the compressive circumferential stress of the cylinder along the radius is shown in Fig. 13. The value of the stress is not the same in the inner and outer layer and $\sigma_\theta / \sigma_\theta^H$ does not equal 1.

The value of the circumferential stress is more than the homogeneous material for $n < 0$ in the inner half of the wall thickness while it is less than that in the outer half. This will be reverse, where $n > 0$. The circumferential stress is almost constant along the radius for $n = 1$. It is observed that in the range of the inner layer of the cylinder, the graphs converge and behave similarly.

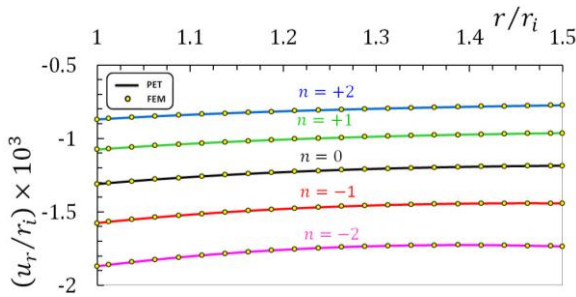


Fig. 14 Distribution of radial displacement, $P_o = 80$ MPa (heterogeneous cylinder)

Fig. 14 shows the distribution of the radial displacement of the cylinder along the wall thickness. u_r / u_r^H does not equal 1 at any point. The value of the radial displacement is more than the homogeneous material for $n < 0$ while it is less than that for $n > 0$. Yet this ratio remains almost constant along the wall thickness.

6.2.3. Internal and external pressure

The nonhomogeneous cylinder is subjected to the internal and external pressures, $P_i = P_o = 80$ MPa.

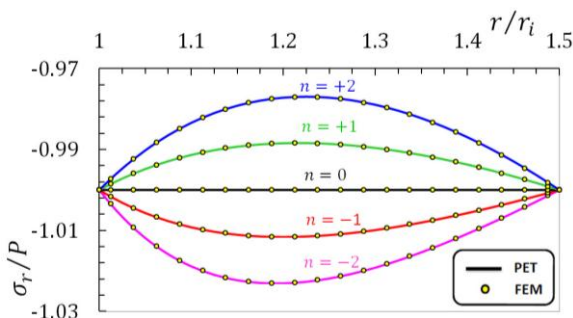


Fig. 15 Distribution of radial stress, $P_i = P_o = 80$ MPa (heterogeneous cylinder)

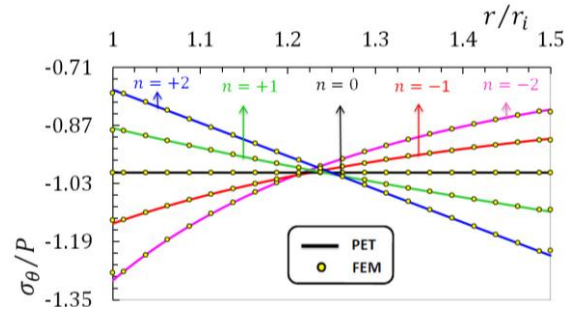


Fig. 16 Distribution of circumferential stress, $P_i = P_o = 80$ MPa (heterogeneous cylinder)

The distribution of the compressive radial stress of the cylinder along the wall thickness is shown in Fig. 15.

The value of the radial stress in the inner and outer layers of the cylinder is the same and $\sigma_r / \sigma_r^H = 1$. In the cylinder wall, the radial stress is more than the radial stress of the homogeneous cylinder for $n < 0$ and is the reverse for $n > 0$. In the homogeneous cylinder, radial stress is almost constant along the wall thickness.

The distribution of the compressive circumferential stress of the cylinder along the wall thickness is shown in Fig. 16. The value of the circumferential stress is not the same in the inner and outer layers of the cylinder and $\sigma_\theta / \sigma_\theta^H$ does not equal 1. The value of the circumferential stress is more than the homogeneous material for $n < 0$ in the inner half of the wall thickness while it is less than that in the outer half. This will be reverse, where $n > 0$. The circumferential stress is almost constant along the radius for $n = 0$. It is observed that in the range of the inner layer of the cylinder, the graphs converge and behave similarly.

Fig. 17 shows the distribution of the radial displacement of the cylinder along the wall thickness. u_r / u_r^H is not 1 at any point. In the cylinder wall, the radial displacement is more than the radial displacement of the

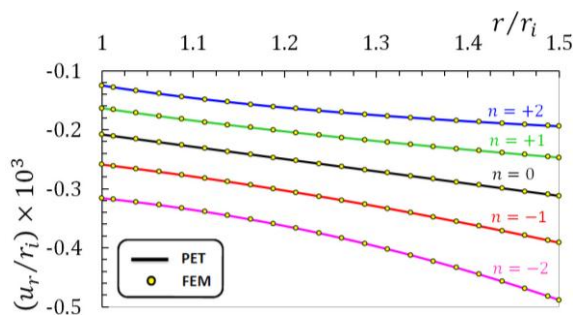


Fig. 17 Distribution of radial displacement, $P_i = P_o = 80$ MPa (heterogeneous cylinder)

Table Comparison of values of effective stress resulting from PET and FEM in the middle layer

Pressure, MPa		$n = -2$	$n = -1$	$n = 0$	$n = +1$	$n = +2$
$P_i = 80$	PET	145.7	154.4	161.7	167.1	170.6
	FEM	143.2	156.2	161.7	165.7	167.6
$P_o = 80$	PET	151.0	161.3	169.7	175.6	179.5
	FEM	151.2	161.4	169.7	175.8	179.5
$P_i = P_o = 80$	PET	32.08	32.04	32	31.90	31.67
	FEM	32.09	32.04	32	31.90	31.69

homogeneous cylinder for $n < 0$ and is the reverse for $n > 0$. In the homogeneous cylinder, radial displacement is almost constant along the wall thickness.

In Table, the values of effective stress resulting from analysis of cylinder through PET and FEM for plane strain condition under internal pressure and/or external pressure in the middle layer are given.

7. Conclusions

It can be concluded that for both positive and negative values of n , the circumferential stress in the non-homogeneous cylinder decreases in one half and increases in the other. In the nonhomogeneous cylinder compared to the homogeneous one, with no external pressure, the radial stress increases and the radial displacement decreases for positive n . For negative n both radial stress and radial displacement increase in the cylinders subjected to external pressure. In contrary, the radial stress and radial displacement decrease for positive n . Decrease or increase of the radial stress and radial displacement depend on $|n|$. According to the requirements for decreasing of the displacement and stress in the nonhomogeneous cylinders, the positive or negative values of n could be applied.

References

1. **Timoshenko, S.P.; Goodier, J.N.** 1970. Theory of Elasticity. 3rd Edition, New York: McGraw-Hill, 395p.
2. **Fukui, Y.; Yamanaka, N.** 1992. Elastic analysis for thick-walled tubes of functionally graded material subjected to internal pressure, JSME International Journal Series I-Solid Mechanics Strength of Materials 35(4): 379-385.
3. **Tutuncu, N.; Ozturk, M.** 2001. Exact solutions for stresses in functionally graded pressure vessels, Composites Part B-Engineering 32(8): 683-686. [http://dx.doi.org/10.1016/S1359-8368\(01\)00041-5](http://dx.doi.org/10.1016/S1359-8368(01)00041-5).
4. **Horgan, C.O.; Chan, A.M.** 1999. The pressurized hollow cylinder or disk problem for functionally graded isotropic linearly elastic materials, Journal of Elasticity, 55(1): 43-59. <http://dx.doi.org/10.1023/A:1007625401963>.
5. **Hongjun, X.; Zhifei, S.; Taotao, Z.** 2006. Elastic analyses of heterogeneous hollow cylinders, Mechanics Research Communications 33(5): 681-691. <http://dx.doi.org/10.1016/j.mechrescom.2006.01.005>.
6. **Zhifei, S.; Taotao, Z.; Hongjun, X.** 2007. Exact solutions of heterogeneous elastic hollow cylinders, Composite Structures 79(1): 140-147. <http://dx.doi.org/10.1016/j.compstruct.2005.11.058>.
7. **Tutuncu, N.** 2007. Stresses in thick-walled FGM cylinders with exponentially-varying properties, Engineering Structures 29(9): 2032-2035. <http://dx.doi.org/10.1016/j.engstruct.2006.12.003>.
8. **Nie, G.J.; Batra, R.C.** 2009. Exact solutions and material tailoring for functionally graded hollow circular cylinders, Journal of Elasticity 99(2): 179-201. <http://dx.doi.org/10.1007/s10659-009-9239-8>.
9. **Nejad, M.Z.; Rahimi, G.H.; Ghannad, M.** 2009. Set of field equations for thick shell of revolution made of functionally graded materials in curvilinear coordinate system, Mechanika 3(77): 18-26.
10. **Ghannad, M.; Nejad, M.Z.** 2010. Elastic analysis of pressurized thick hollow cylindrical shells with clamped-clamped ends, Mechanika 5(85): 11-18.

Mehdi Ghannad, Mohammad Zamani Nejad

AUKŠTO SLĖGIO STORASIENIO KEVALO
PAGAMINTO IŠ NEVIENALYTĖS AUKŠTOS
KOKYBĖS MEDŽIAGOS PILNAS TAMPRUSIS
SPRENDIMAS

R e z i u m ė

Laikant, kad tamprumo modulis radialine kryptimi kinta netiesiškai, o Puasono koeficientas yra pastovus, remiantis plokštumos tamprumo teorija sudarytos asimetrinio storasienio cilindro kevalo, pagaminto iš nevienalytės aukštos kokybės medžiagos ir apkrauto vidiniu bei išoriniu slėgiu, svarbiausios bendrosios lygtys. Sudarytos Navje lygtys realioms, sudvejintoms ir kompleksinėms šaknims analitiškai skaičiuoti plokščiosios deformacijos ir plokščiųjų įtempių atvejais. Baigtinių elementų metodu apskaičiuota radialinių apskritiminių įtempių ir radialinių poslinkių pasiskirstymas priklausomai nuo nevienalytiškumo konstantų yra palygintas su vienalytės medžiagos įtempimų ir radialinių poslinkių pasiskirstymu, o rezultatai pavaizduoti grafiškai.

M. Ghannad, M. Z. Nejad

COMPLETE ELASTIC SOLUTION OF PRESSURIZED
THICK CYLINDRICAL SHELLS MADE OF
HETEROGENEOUS FUNCTIONALLY GRADED
MATERIALS

S u m m a r y

Assuming the Young's modulus vary nonlinearly in the radial direction, and the Poisson's ratio is constant, on the basis of plane elasticity theory (PET), the governing equations for axisymmetric thick cylindrical shells made of nonhomogeneous functionally graded materials (FGMs) subjected to internal and external pressure in general case are derived. The analytical solution of the Navier equations for real, double and complex roots and plane strain, plane stress and the cylinder with closed ends conditions are obtained. The radial stress, circumferential stress and radial displacement distributions depending on an inhomogeneity constant are compared with those of the homogeneous case, the solution using finite element method (FEM) and presented in the form of graphs.

Keywords: elastic solution, thick cylindrical shell, heterogeneous functionally graded materials.

Received June 14, 2011

Accepted November 15, 2012